Hydrogen Generation

DOI: 10.1002/anie.201102917

Computational Evidence for Hydrogen Generation by Reductive Cleavage of Water and α-H Abstraction on a Molybdenum Complex[**]

*Jun Li and Kazunari Yoshizawa**

Owing to the increasing global energy demand and declining oil resources, hydrogen has attracted extensive attention as a good candidate for a clean, sustainable fuel.[1] Besides heterogeneous catalysts, some homogenous systems have also been developed, with inspiration from hydrogenase enzymes, for catalytic generation of H_2 from water.[2] In 2010, Karunadasa, Chang, and Long reported a novel and interesting electrocatalytic cycle for reduction of water to form H_2.[3] They achieved H_2 evolution from the reaction of $[(PY5Me_2)MoO](PF_6)_2$ ($PY5Me_2$ = 2,6-bis[1,1-bis(2-pyridyl)ethyl]pyridine) with water in electrolysis experiments. Their discovery established a distinct paradigm for producing H_2 from water. Elucidation of the mechanism and energetics of this reaction is important for further development of active complexes for water reduction and a better understanding of the processes occurring on hydrogenase enzymes.

On the basis of detailed DFT calculations, we propose possible electrocatalytic cycles for H_2 generation from water starting with $[(PY5Me_2)MoO]^{2+}$, as schematically illustrated in Scheme 1. All calculations were carried out with the Gaussian 09 program suite.[4] The unrestricted PBE1PBE hybrid functional[5] was adopted after careful selection. The geometry of each species was optimized in aqueous phase by incorporating solvent effects with the polarizable continuum model (PCM).[6] Two possible spin states were examined for most species, and for a few stationary points three spin states were checked. Other computational details are described in the Supporting Information.

The Mo^{IV} oxo complex $[(PY5Me_2)MoO]^{2+}$ (**1**) was identified in the singlet state. As shown in Figure 1, the Mo–O bond length in **1** is calculated to be 1.685 Å, identical to the experimentally measured value.[3] One- and two-electron reductions of **1** give birth to $[(PY5Me_2)MoO]^{+}$ (**2**) and $[(PY5Me_2)MoO]$ (**3**), respectively. Complex **2** adopts the doublet state, and **3** the triplet state; the triplet–singlet energy gap of **3** is only 1.3 kcal mol^{-1}. Computed redox potentials for $[(PY5Me_2)MoO]^{2+/+}$ and $[(PY5Me_2)MoO]^{+/0}$ couples are −0.69 and −1.45 V versus standard hydrogen electrode (SHE), respectively. The calculated Mo–O bond lengths in **2** and **3** of 1.756 and 1.813 Å, respectively, indicate that the Mo–O bond is weakened step by step during the reduction. The reaction of **1** with H_2O is energetically unfavorable, being endergonic by 24.7 kcal mol^{-1} with an activation energy of 38.0 kcal mol^{-1}. Detailed results are given in the Supporting Information. In the following, we discuss the reactions of **2** with H_2O and **3** with H_2O. Gibbs free-energy profiles for these two reactions are presented in Figures 2 and 3, respectively. Optimized geometries of the species involved in the reaction of **2** with H_2O are shown in Figure 1, and other optimized geometries are provided in the Supporting Information (Figure S4).

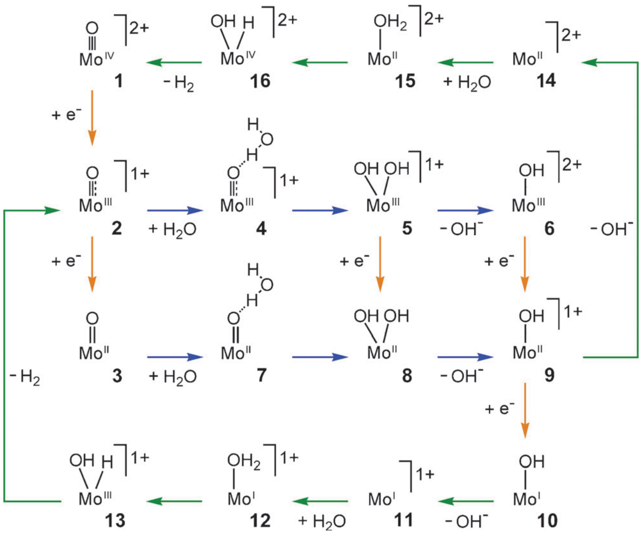

Scheme 1. Possible catalytic cycles for H_2 generation from water starting with $[(PY5Me_2)Mo^{IV}O]^{2+}$. The $PY5Me_2$ ligand is omitted.

When **2** reacts with H_2O, precursor complex **4** is firstly formed, in which H_2O is bonded to the oxo ligand through a hydrogen bond. This step is endergonic by 6.6 kcal mol^{-1}. Next, the bound H_2O is deprotonated through nucleophilic attack by the oxo ligand, and dihydroxo complex $[(PY5Me_2)Mo(OH)_2]^{+}$ (**5**) is formed. Complex **4** is in the doublet state, but **5** adopts the quartet state; the transformation of **4** into **5** goes through a doublet transition state (**TS4/5**). This step is slightly endergonic by 1.4 kcal mol^{-1} and has a moderate activation energy of 20.7 kcal mol^{-1}. Subsequently, an OH^- anion can be eliminated from **5**, and monohydroxo complex $[(PY5Me_2)Mo(OH)]^{2+}$ (**6**) is pro-

---

[*] Dr. J. Li, Prof. Dr. K. Yoshizawa
Institute for Materials Chemistry and Engineering
International Research Centre for Molecular Systems
Kyushu University, Fukuoka 819-0395 (Japan)
E-mail: kazunari@ms.ifoc.kyushu-u.ac.jp

[**] K.Y. acknowledges Grants-in-Aid (Nos. 18GS0207 and 22245028) for Scientific Research from Japan Society for the Promotion of Science (JSPS) and the Ministry of Education, Culture, Sports, Science and Technology of Japan (MEXT), the Nanotechnology Support Project of MEXT, the MEXT Project of Integrated Research on Chemical Synthesis, the Kyushu University Global COE Project "Future Molecular Systems", and CREST of the Japan Science and Technology Cooperation for their support of this work.

Supporting information for this article is available on the WWW under http://dx.doi.org/10.1002/anie.201102917.

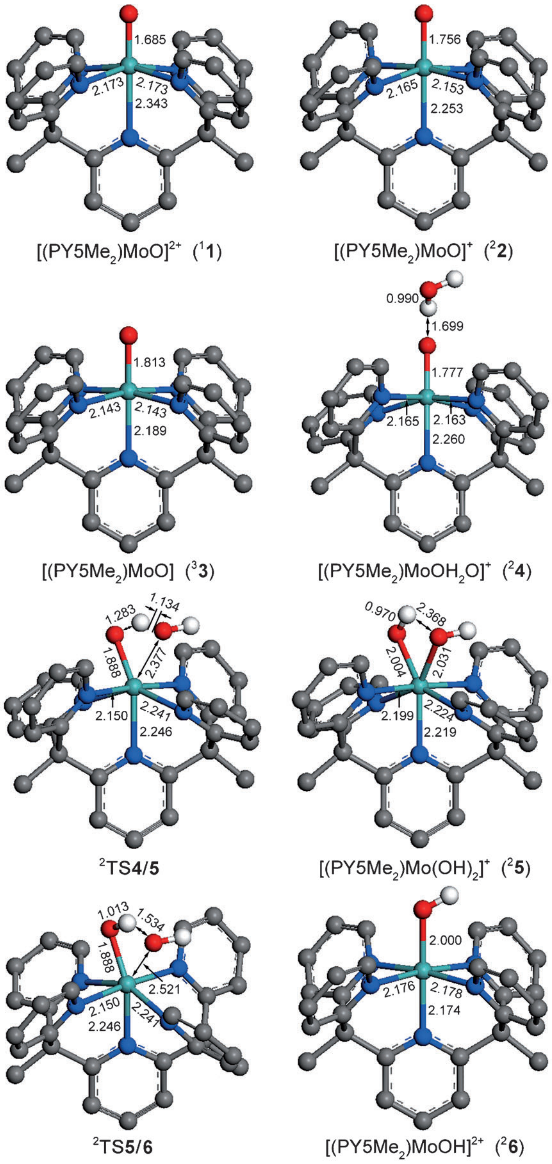

Figure 1. Optimized geometries of Mo oxo complexes **1**–**3**, and the species involved in the reaction of **2** with H$_2$O and the elimination of OH$^-$. Mo, O, N, C, and H atoms are represented by green, red, blue, gray, and white, respectively. H atoms on the PY5Me$_2$ ligand are omitted for clarity. Selected distances are given in Å. The superscript indicates the spin multiplicity of each species (1, 2, 3, and 4 for the singlet, doublet, triplet, and quartet state, respectively).

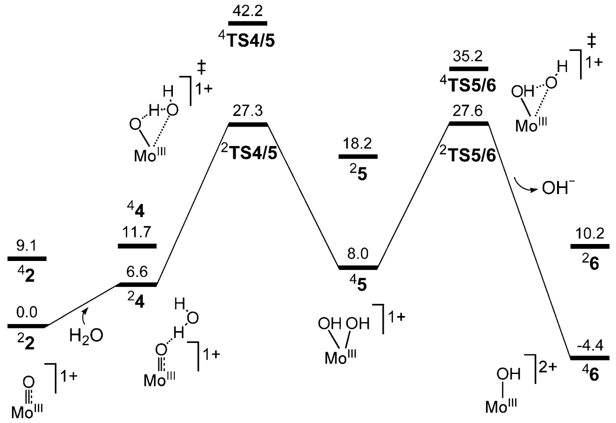

Figure 2. Free-energy (298.15 K, in kcal mol^{-1}) profile for the reaction of **2** with H$_2$O and the elimination of an OH$^-$ anion.

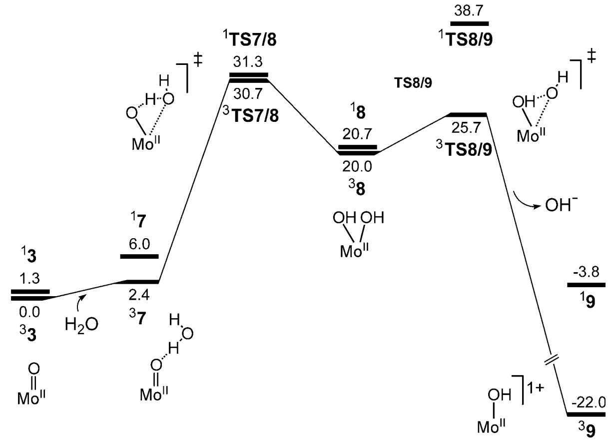

Figure 3. Free-energy (298.15 K, in kcal mol^{-1}) profile for the reaction of **3** with H$_2$O and the elimination of an OH$^-$ anion.

duced. Note that **5** and **6** are both in the quartet states, but the transition state in this step (**TS5/6**) is in the doublet state. This step is exergonic by 12.4 kcal mol^{-1} and the activation energy is 19.6 kcal mol^{-1}. The further elimination of OH$^-$ from **6** is thermodynamically unfeasible, because it is endergonic by 29.6 kcal mol^{-1}.

The reaction of **3** with H$_2$O is somewhat like the reaction of **2** with H$_2$O, but the former proceeds on the triplet surface, although the triplet–singlet energy gaps of some stationary points are small. The overall reaction is exergonic by 22.0 kcal mol^{-1} and the highest barrier on the whole potential energy surface is 30.7 kcal mol^{-1}. The activation energy (28.3 kcal mol^{-1}) for deprotonation of H$_2$O in **7** is higher than that for the deprotonation of H$_2$O in **4**, because **TS7/8** and **TS4/5** are both post-transition states, and the energy of **8** relative to **7** is much higher than that of **5** relative to **4**. Hence, the stronger nucleophilicity of Mo^{II}(oxo) in **3** does not play a major role. Elimination of an OH$^-$ anion from **8** is facile; it is strongly exergonic by 42.0 kcal mol^{-1} with a low activation energy of 5.7 kcal mol^{-1}. Elimination of the second OH$^-$ anion is not so energetically favorable, because it is endergonic by 16.5 kcal mol^{-1}.

One-electron reduction of **5** yields **8**, and reduction of **6** yields **9**. In addition, **9** can be reduced to Mo^{I} monohydroxo complex [(PY5Me$_2$)MoOH] (**10**). We mentioned above that one- and two-electron reductions of **1** lead to **2** and **3**, respectively. All computed redox potentials for the possible couples involved in this electrochemical system are collected in Table 1.[7] Karunadasa, Chang, and Long observed two half-wave potentials of this reaction system in aqueous KCl solution at $E_{1/2} = -0.58$ and -1.06 V versus SHE,[3] and assigned them to [(PY5Me$_2$)MoO]$^{2+/+}$ and [(PY5Me$_2$)MoO]$^{+/0}$ couples. Computed redox potentials for [(PY5Me$_2$)MoO]$^{2+/+}$ and [(PY5Me$_2$)MoO]$^{+/0}$ couples are

Table 1: Computed redox potentials [V vs. SHE] for the possible couples in this investigated electrochemical system.

Redox couple	$[(PY5Me_2)MoO]^{2+/+}$	$[(PY5Me_2)MoO]^{+/0}$	$[(PY5Me_2)Mo(OH)_2]^{+/0}$	$[(PY5Me_2)MoOH]^{2+/+}$	$[(PY5Me_2)MoOH]^{+/0}$
redox potential	−0.69	−1.45	−1.94	−0.68	−1.40

close to those for $[(PY5Me_2)MoOH]^{2+/+}$ and $[(PY5Me_2)MoOH]^{+/0}$ couples, respectively. If reduction of **1** to **2** and **3** occurs, then reduction of **6** to **9** and **10** can take place as well.

Once **10** is formed, elimination of OH^- releases the Mo^I site ($[(PY5Me_2)Mo]^+$ (**11**)). This step is endergonic by 5.1 kcal mol^{-1}. The Mo^I site is active enough to generate H_2 by reductive cleavage of water and subsequent α-H abstraction. Optimized geometries of all species involved in this process are presented in Figure 4, and the Gibbs free-energy profile for this process is shown in Figure 5. Coordination of H_2O at this Mo^I site leads to formation of aquo complex $[(PY5Me_2)Mo(OH_2)]^+$ (**12**), which is endergonic by 1.4 kcal mol^{-1}. Oxidative addition of H_2O to Mo^I forms hydrido hydroxo complex $[(PY5Me_2)MoH(OH)]^+$ (**13**). Cleavage of H_2O into hydride and hydroxide is endergonic by 5.4 kcal mol^{-1} with a moderate activation energy of 24.9 kcal mol^{-1}. Finally, the hydride will capture the proton of the hydroxide ligand to generate H_2. At the same time, Mo^{III} oxo complex **2** is regenerated. This step is exergonic by 18.1 kcal mol^{-1} and the activation energy is moderate (23.4 kcal mol^{-1}). All of these steps occur on the doublet surface. The whole process of water reduction on Mo^I to form H_2 and **2** is exergonic by 11.3 kcal mol^{-1} and has an overall barrier of 30.2 kcal mol^{-1}.

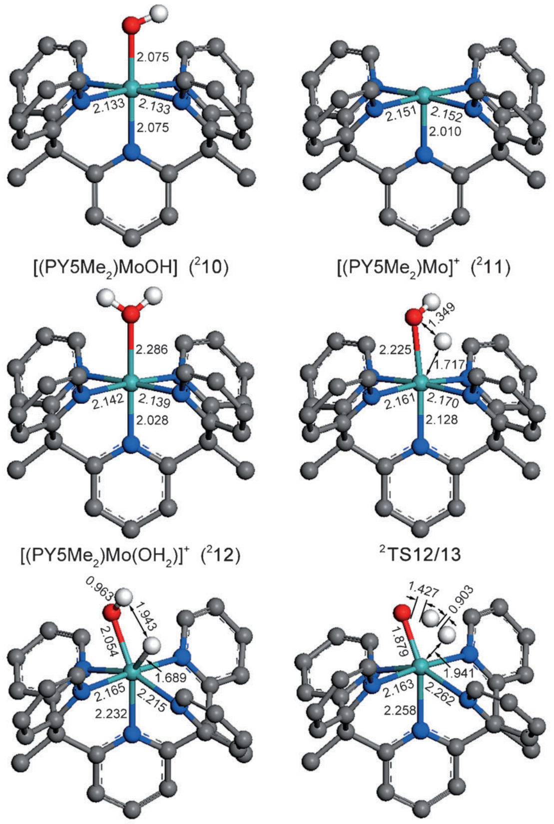
$[(PY5Me_2)MoOH]$ (^{2}10) $[(PY5Me_2)Mo]^+$ (^{2}11)
$[(PY5Me_2)Mo(OH_2)]^+$ (^{2}12) ^{2}TS12/13
$[(PY5Me_2)MoH(OH)]^+$ (^{2}13) ^{2}TS13/2

Figure 4. Optimized geometries of the species involved in water reduction to form H_2 on Mo^I. Selected distances are given in Å.

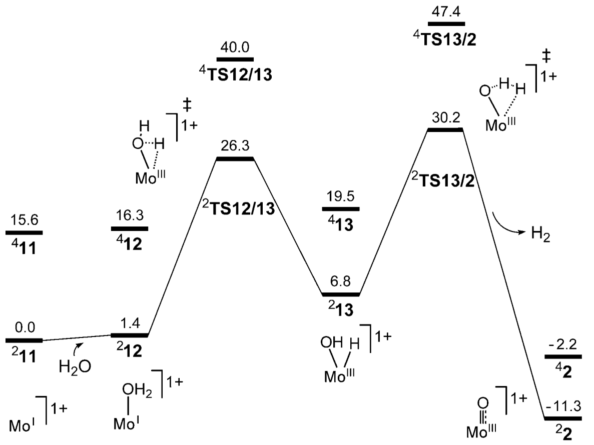

Figure 5. Free-energy (298.15 K, in kcal mol^{-1}) profile for the reduction of water to form H_2 on Mo^I.

We also considered the possibility of water reduction to H_2 on Mo^{II}. The Gibbs free-energy profile for H_2 generation on Mo^{II} is depicted in Figure 6, and optimized geometries of the species involved in this process are given in the Supporting Information (Figure S5). The whole process is exergonic by 9.1 kcal mol^{-1} and has an overall barrier of 42.9 kcal mol^{-1}. This barrier is higher than that for reduction of water on Mo^I, that is, Mo^{II} is less active.

All possible reaction steps depicted in Scheme 1 have been already explored. On the basis of the calculations described above, we suggest that the most likely cycle for the

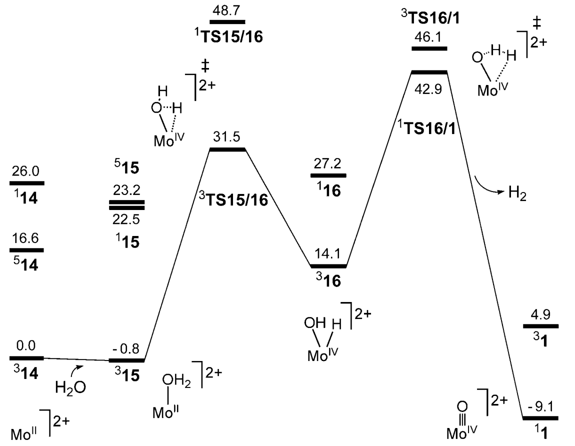

Figure 6. Free-energy (298.15 K, in kcal mol^{-1}) profile for the reduction of water to form H_2 on Mo^{II}.

generation of H_2 from water in this electrochemical system is **2**→**4**→**5**→**6**→**9**→**10**→**11**→**12**→**13**→**2**. In this cycle **10**→**11**→**12**→**13**→**2**→**4**→**5**→**6** is a thermochemical process and **6**→**9**→**10** is an electrochemical process. Overall, this catalytic cycle can be represented by Equation (1).

$$2\,H_2O + 2\,e^- \rightarrow H_2 + 2\,OH^- \qquad (1)$$

This process is distinct from the mechanisms previously proposed for H_2 evolution on hydrogenases[8] and some molecular catalysts,[9] in which H_2 is generated by proton reduction. Interestingly, in this process the two H atoms of the formed H_2 come from an H_2O molecule [Eq. (2)].

$$H_2O + 2\,e^- \rightarrow OH^- + H^- \rightarrow O^{2-} + H_2 \qquad (2)$$

We additionally studied the reaction of H_2O with MoO^+ species (without the $PY5Me_2$ ligand) and reduction of H_2O on bare Mo^+ ion. Detailed results are provided in the Supporting Information. The reaction of H_2O with MoO^+ to form $Mo(OH)_2{}^+$ is very facile, being exergonic by 10.7 $kcal\,mol^{-1}$ with a barrier of 11.9 $kcal\,mol^{-1}$, but the elimination of OH^- is thermodynamically unfavorable, since even the first step is endergonic by 35.3 $kcal\,mol^{-1}$. The production of H_2 by H_2O reduction on bare Mo^+ ion is exergonic by 19.7 $kcal\,mol^{-1}$ and involves an overall barrier of 16.9 $kcal\,mol^{-1}$. Accordingly, when a suitable ligand is chosen, H_2 can be generated from H_2O on Mo^I. The major obstacle to accomplishing a catalytic cycle is elimination of OH^- anions.

Karunadasa, Chang, and Long also reported production of H_2 from the reactions of $[(PY5Me_2)Mo(CF_3SO_3)]^+$ with H_2O and $[(PY5Me_2)MoI]^{2+}$ with H_2O.[3] These two reactions can take place because the active Mo^{II} site is formed during the reaction. Detailed results are presented in the Supporting Information.

It is interesting that generation of H_2 on all three active complexes occurs through reductive cleavage of H_2O and subsequent α-H abstraction. This has long been considered as a possible mechanism for reduction of water to H_2, but a clear example was not established.[10] Now our computational results, based on the experimental facts, reveal that H_2 production by reductive cleavage of H_2O and subsequent α-H abstraction on $[(PY5Me_2)Mo]^+$ is energetically favorable. H_2 formation by a similar mechanism occurring on $[(PY5Me_2)Mo]^{2+}$ is also possible, although less favorable. These findings broaden the understanding of mechanisms for water reduction and may be helpful for developing more active or applicable catalysts for H_2 generation from H_2O.

Received: April 28, 2011
Revised: August 2, 2011

Keywords: density functional calculations · hydrogen generation · molybdenum · reaction mechanisms · water reduction

---

[1] J. A. Turner, *Science* **2004**, *305*, 972–974.

[2] a) S. W. Kohl, L. Weiner, L. Schwartsburd, L. Konstantinovski, L. J. W. Shimon, Y. Ben-David, M. A. Iron, D. Milstein, *Science* **2009**, *324*, 74–77; b) F. Gärtner, B. Sundararaju, A.-E. Surkus, A. Boddien, B. Loges, H. Junge, P. Dixneuf, M. Beller, *Angew. Chem.* **2009**, *121*, 10147–10150; *Angew. Chem. Int. Ed.* **2009**, *48*, 9962–9965; c) K. Yamauchi, S. Masaoka, K. Sakai, *J. Am. Chem. Soc.* **2009**, *131*, 8404–8406; d) P. Zhang, M. Wang, Y. Na, X. Li, Y. Jiang, L. Sun, *Dalton Trans.* **2010**, *39*, 1204–1206; e) F. Wang, W.-G. Wang, X.-J. Wang, H.-Y. Wang, C.-H. Tung, L.-Z. Wu, *Angew. Chem.* **2011**, *123*, 3251–3255; *Angew. Chem. Int. Ed.* **2011**, *50*, 3193–3197; f) H. Krassen, S. Ott, J. Heberle, *Phys. Chem. Chem. Phys.* **2011**, *13*, 47–57.

[3] H. I. Karunadasa, C. J. Chang, J. R. Long, *Nature* **2010**, *464*, 1329–1333.

[4] Gaussian09 (Revision A.02): M. J. Frisch et al., see the Supporting Information.

[5] M. Ernzerhof, J. P. Perdew, *J. Chem. Phys.* **1998**, *109*, 3313–3320.

[6] a) S. Miertus, E. Scrocco, J. Tomasi, *Chem. Phys.* **1981**, *55*, 117–129; b) S. Miertus, J. Tomasi, *Chem. Phys.* **1982**, *65*, 239–245.

[7] See the Supporting Information for detailed computational methods, results, and discussion.

[8] a) Z. Cao, M. B. Hall, *J. Am. Chem. Soc.* **2001**, *123*, 3734–3742; b) M. Y. Darensbourg, E. J. Lyon, X. Zhao, I. P. Georgakaki, *Proc. Natl. Acad. Sci. USA* **2003**, *100*, 3683–3688; c) T. Zhou, Y. Mo, A. Liu, Z. Zhou, K. R. Tsai, *Inorg. Chem.* **2004**, *43*, 923–930; d) S. Trohalaki, R. Pachter, *Int. J. Hydrogen Energy* **2010**, *35*, 5318–5331.

[9] a) M. T. M. Koper, E. Bouwman, *Angew. Chem.* **2010**, *122*, 3810–3812; *Angew. Chem. Int. Ed.* **2010**, *49*, 3723–3725; b) T. M. McCormick, B. D. Calitree, A. Orchard, N. D. Kraut, F. V. Bright, M. R. Detty, R. Eisenberg, *J. Am. Chem. Soc.* **2010**, *132*, 15480–15483.

[10] a) N. S. Lewis, D. G. Nocera, *Proc. Natl. Acad. Sci. USA* **2006**, *103*, 15729–15735; b) D. G. H. Hetterscheid, J. I. van der Vlugt, B. de Bruin, J. N. H. Reek, *Angew. Chem.* **2009**, *121*, 8324–8327; *Angew. Chem. Int. Ed.* **2009**, *48*, 8178–8181; c) W. E. Piers, *Organometallics* **2011**, *30*, 13–16.